Supporting Information

Paeng et al. 10.1073/pnas.1424636112

SI Materials and Methods

Synthesis and Characterization of BODIPY268. The new asymmetric BODIPY268 was obtained by the condensation of pyrrole 2-carboxaldehyde and 2-phenyl-1H-pyrrole (Fig. S1), as suggested by synthesis of a similar molecule (1).

Pyrrole 2-carboxaldehyde (100 mg, 0.95 mmol) was dissolved in dichloromethane (5 mL) and cooled to 0 °C under argon atmosphere. Then, 2-phenyl-1H-pyrrole (136 mg, 0.95 mmol) was added to the reaction mixture and stirred for 15 min, followed by slow dropwise addition of $POCl_3$ (88.5 μL, 0.95 mmol). The reaction mixture was stirred at 0 °C for 3 h and at room temperature for another 3 h. Then, 0.4 mL (2.85 mmol) of triethylamine and 0.35 mL (2.85 mmol) BF_3OEt_2 were added and stirred for 3 h. Water was added to the reaction mixture, and the organic phase was extracted three times. To remove remaining water in the organic phase, the sample was dried over $MgSO_4$. The residue was purified by silica gel column chromatography with a mobile phase of hexane:EtOAc = 7:1 three times followed by toluene:hexane = 5:1.

High resolution mass spectrometry (fast atom bombardment). Calculated for $C_{15}H_{11}N_2F_2B$ *m/z* 268.0986; measured *m/z* 268.1715.

^{1}H NMR (400 MHz, $CDCl_3$, δ in parts per million), 8.00–7.98 (m, 2H; Ar), 7.82 (br. s, 1H, *n* = CH), 7.53–7.50 (m, 3H; Ar), 7.38 (s, 1H), 7.24 (d, J = 4.4 Hz, 1H), 7.11 (d, J = 4.0 Hz, 1H), 6.75 (d, J = 4.4 Hz, 1H), 6.55 (d, J = 4.0 Hz, 1H).

Fig. S2 shows normalized absorption and fluorescence spectra of BODIPY268. The vertical dashed line indicates the 532-nm line where the probe molecules were excited in the experiment. Both absorbance and emission spectra were acquired in toluene. Quantum yield was determined to be close to unity using Rhodamine 6G as a reference. The extinction coefficient was measured to be 53,000 $cm^{-1}{\cdot}M^{-1}$. BODIPY268 in toluene shows maximum excitation and emission at 531.4 nm and 546.0 nm, respectively, a Stokes shift of ∼15 nm. Photostability was investigated by comparing the survival time of probes in polystyrene excited with ∼200 W/cm^2, a typical excitation power density for single-molecule measurements. Median survival time was ∼1,500 s, comparable to Rhodamine 6G (∼1,500 s) and tbPDI (*N,N′*-bis(2,5-tert-butylphenyl)-3,4,9,10-perylene dicarboximide) (∼2,000 s).

Heating Correction. Because of the relatively high power density excitation used in single-molecule measurements to assure sufficient signal-to-noise, sample heating relative to the set temperature can occur. Actual temperature of samples used in this report was estimated using low-power measurements of the brighter probe molecule tbPDI (*N,N′*-bis(2,5-tert-butylphenyl)-3,4,9,10-perylenedicarboximide) in *o*-terphenyl. For continuous and shuttered movies, the dependence of the rotational correlation time on the excitation power was measured to be –0.01 decades per milliwatt and –0.0012 decades per milliwat, respectively. The changes in rotational correlation time were converted to temperature changes using the temperature dependence of the dielectric relaxation time of *o*-terphenyl (2). When the sample was illuminated with 10 mW (100 W/cm^2) at T_g + 10 K, the actual sample temperature was ∼0.4 K higher than the set temperature for a continuous movie and ∼0.05 K higher than the set temperature for a shuttered movie. The heating-corrected temperatures are used in Fig. 1*D*. In all other instances when referring to temperature, set temperature rather than heating-corrected temperature is denoted for convenience.

SI Results and Discussion

Combined Frame Rate Studies. All time domain measurements, including the single-molecule rotation measurements described here, have a given dynamic range. For experiments measuring relaxation times in systems with homogeneous dynamics, where a narrow relaxation time distribution is expected, dynamic range limitations are not a significant concern. However, in a dynamically heterogeneous system, limited dynamic range can result in missing a portion of the relaxation times in the system. In the particular experiments reported here, linear dichroism data from single BODIPY268 molecules in *o*-terphenyl at a given temperature were collected at a single frame rate. The maximum dynamical window for a single frame rate measurement is expected to be roughly 2 decades. This is set by the assumption that the minimum points needed to fit an ACF is 2 points per τ_{fit}, setting the minimum time reported as one tenth of that associated with the median if the median frame rate is set to be 20 points per τ_{fit}. We restrict trajectory length to >10τ_{fit}, thus automatically eliminating molecules with >200 points per τ_{fit} and setting the maximum time reported as 10 times the median. Given that the dynamical window associated with a single frame rate measurement is similar to the maximum rotational time distribution found in this study, to test whether these single frame measurements reported the full range of rotation times in the system, measurements at a particular temperature were also taken as a function of frame rate. The combined frame rate distribution was constructed and compared with the distribution acquired by single frame rate measurements.

To construct a frame rate combined histogram, data from two different temperatures (244.5 K and 247.5 K) were used. At 244.5 K, frame rate was varied from 37.5 times faster to 3 times slower than the typical single frame rate, set such that frame rate yielded 15–20 frames per τ_{fit}. At 247.5 K, frame rate was varied from 3 times faster to 27 times slower than the typical single frame rate. By combining histograms from these two temperatures, the dynamic window was increased by a factor of ∼1,000, effectively covering 5 decades in time. For movies at each frame rate, only molecules with rotation times within a narrow range (0.48 decade) were selected and analyzed to assure good fits to the relaxations and to mimic frequency sweep measurements. The fraction of molecules that met the criteria relative to the total number of identified molecules was accounted for in constructing the frame rate combined histogram. For instance, if the standard frame rate was set to 20 points per τ_{fit} and the frame rate was varied by factor of 3, only molecules with frame rate greater than 11.55 and less than 34.64 points per τ_{fit} were analyzed. This prevented overcounting molecules that may otherwise be present in multiple movies of different frame rate.

Fig. S3 compares τ_{fit} distributions obtained from a single frame rate measurement and a frame rate combined measurement. This similarity shows that single frame rate movies are sufficient to return the full range of rotational relaxation times present in the system so long as the frame rate is chosen appropriately.

Building Reference ILT and ILT-Built Distributions. A stretched exponential function can be written as a sum of exponential functions.

$$e^{-\left(t/\tau_{fit}\right)^{\beta}} = \int_{-\infty}^{\infty} P\left(\log\tau;\tau_{fit},\beta\right)\cdot e^{-t/\tau} d\log\tau. \qquad \textbf{[S1]}$$

Here $P(\log\tau;\tau_{fit},\beta)$ is the normalized probability density function of relaxation times obtained from exponential decays.

Mathematically, Eq. **S1** is the ILT, and there exist numerical expressions for the probability density function. In principle,

these functions can be obtained numerically for any τ_{fit} and β values. However, at high and low values of the reduced rate $s = \tau_{fit}/\tau$, there are often convergence problems, making it impractical to use the numerical expressions to generate the probability distribution for those τ_{fit} and β values. To circumvent this problem, we built a set of reference distributions for $\tau_{fit} = 1$ and β ranging from 0.20 to 0.99 in 0.01 steps and used these reference distributions to approximate the distribution for any given τ_{fit} and β value.

Below are the numerical expressions for the probability density function written in s space (3, 4).

$$e^{-(\lambda_0 \cdot t)^\beta} = \int_0^\infty P(s,\beta) \cdot e^{-s\cdot\lambda_0 \cdot t} ds, \quad \text{where} \quad s = \lambda/\lambda_0 = \tau_{fit}/\tau \qquad \textbf{[S2]}$$

$$P(s,\beta) = \frac{1}{\pi} \int_0^\infty e^{-u^\beta \cdot \cos(\pi\beta/2)} \cdot \cos\left[su - u^\beta \cdot \sin(\pi\beta/2)\right] du \qquad \textbf{[S3]}$$

$$P(s,\beta) = \frac{1}{\pi} \int_0^\infty e^{-su} \cdot e^{-u^\beta \cdot \cos(\pi\beta)} \cdot \sin\left[u^\beta \cdot \sin(\pi\beta)\right] du. \qquad \textbf{[S4]}$$

Given that measured distributions of rotational correlation times have been nearly log normal, we wish to express the distribution of relaxation times on a logarithmic scale. As such, we transform Eq. **S2** into log(τ) space, as shown in Eq. **S5**.

$$\begin{aligned}\int_0^\infty P(s,\beta) \cdot e^{-s\cdot\lambda_0 \cdot t} ds &= \int_\infty^0 P\left(\frac{\tau_{fit}}{\tau},\beta\right) \cdot e^{-t/\tau} \cdot \left(-\frac{\tau_{fit}}{\tau^2}\right) d\tau \\ &= \int_{-\infty}^\infty P\left(\frac{\tau_{fit}}{\tau},\beta\right) \cdot \frac{\tau_{fit} \cdot \ln 10}{\tau} \cdot e^{-t/\tau} d\log\tau \\ &= \int_{-\infty}^\infty P(\log\tau; \tau_{fit}, \beta) \cdot e^{-t/\tau} d\log\tau. \end{aligned} \qquad \textbf{[S5]}$$

In principle, both Eqs. **S3** and **S4** give the probability distribution; however, in practice, Eq. **S3** converges better in the $0.5 < \beta < 1.0$ range and Eq. **S4** in the $0.2 \le \beta \le 0.5$ range. In any case, computer-generated $P(\log\tau; \tau_{fit}, \beta)$ functions are often still inaccurate in the fast time regime. Each $P(\log\tau; \tau_{fit}, \beta)$ distribution was compared with the distribution generated by the CONTIN procedure (5) performed on a stretched exponential function with the same β value. The CONTIN procedure is a commonly used constrained least squares fitting algorithm to estimate the distribution of underlying exponential decays from experimental stretched exponential data. The fast time tail of the $P(\log\tau; \tau_{fit}, \beta)$ distribution was approximated from this procedure to complete the distribution. After this set of operations, the relaxation function generated from a reference distribution constructed for a particular β value could be fit to the original stretched exponential function with the β value from the fit with less than 1% error relative to its initial value.

Fig. S4 shows examples of the reference distributions. The blue open symbols are the original stretched exponential functions with β as indicated in the plot. Black solid curves are reference distributions $P(\log\tau; \tau_{fit}, \beta)$ generated from the stretched exponential function as described above. The red lines are the relaxation functions generated from the reference distributions, which match very well with the original stretched exponential functions, thus validating the obtained distributions $P(\log\tau; \tau_{fit}, \beta)$.

Using this set of reference ILT distributions, ILT-built distributions were constructed from each experimental data set. Each single-molecule ACF within a data set was fit to a stretched exponential, and, according to its fitted β value, a reference distribution was chosen and shifted in time by the fitted τ_{fit} value. This process was repeated for all single-molecule ACFs, and the distributions were added and normalized by the area under the distribution to produce an ILT-built distribution for each data set.

From the ILT-built distribution, an ACF was constructed by summing exponential decay functions weighted by the ILT-built distribution. β_{ILT} is the fit value of that decay function to the stretched exponential function and is found to be within 0.01 of the β_{QE} for each data set.

Contributions of Molecules with Specific β Values to the ILT-Built Distribution. To examine how molecules with stretched exponential relaxations with different β values contribute to the overall relaxation time distribution, ILT-built distributions were produced for molecules with β values in distinct ranges (as obtained from single frame rate movies). An ILT-built distribution for molecules with β values ranging from 0.60 to 0.70 was produced first, and the range of β values was gradually expanded (Fig. S5*A*). Each such distribution was compared with the ILT distribution associated with $\beta = 0.65$. Fig. S5*A* shows the residuals associated with subtracting the ILT distribution for $\beta = 0.65$ from each ILT-built distribution. The area mismatch between the distributions was calculated from these residuals and is plotted in Fig. S5*B*. The mismatch stays relatively constant until the β value range spans beyond 0.40–0.90, which covers ~80% of the total molecules assessed. Even with all β values included (Fig. 2*B*), the mismatch does not exceed 11%. Triangles and squares in Fig. S5*B*, *Inset*, show the mismatch calculated from the ILT-built distribution produced by including molecules with β values at the lower and higher ends of the β distribution.

To further understand the sensitivity of the obtained distribution, ILT-built distributions were also generated from sets of molecules excluding molecules with β values in the middle of the β distribution. ILT-built distributions generated without molecules demonstrating β values in the 0.60–0.70 and 0.50–0.80 ranges are presented and compared with the distribution associated with $\beta = 0.65$ (Fig. S5*C*). These ILT-built distributions also match the distribution from a $\beta = 0.65$ stretched exponential reasonably well. This is in contrast to a distribution generated from the simple addition of two ILT distributions at $\beta = 0.45$ and $\beta = 0.85$, which has gross discrepancy from the ILT distribution associated with $\beta = 0.65$ (Fig. S5*D*). This suggests that the ILT-built distribution generated by single molecules with relaxations yielding stretched exponentials with high and low β values compensate each other to produce the ILT-built distribution resembling that associated with the ensemble β.

Time for Ergodicity Recovery. Fig. 4*B* shows that β values reach the ensemble β value by ~200 times the structural relaxation time of *o*-terphenyl. To describe the dependence of β on trajectory length, data were fit to an arbitrary function expressed below that assumes a starting value of 1 and convergence to a certain value, β_∞. Here τ_t is the trajectory length at which the β value reaches 63.2% of the β_∞ value.

$$\beta(\text{trajectory}) = (1 - \beta_\infty) \cdot \exp[-(\text{trajectory}/\tau_t)^\alpha] + \beta_\infty. \qquad \textbf{[S6]}$$

As seen in Fig. 4, β varies with trajectory length in a manner that is well described by this function with $\beta_\infty = 0.61$ and $\alpha = 1.2$, which shows that β converges in roughly 1 decade. However, this measure may not be sensitive to rare environments, and full convergence may take somewhat longer. Another way to estimate the time required for ergodicity recovery is to follow the

width of the β and τ_{fit} distributions as a function of trajectory length (Fig. S6). Fig. S6 shows how FWHM of the β and τ_{fit} distributions change with trajectory length, with FWHM obtained by fitting the distributions presented in Fig. 3 to Gaussian functions. The width of the β and τ_{fit} distributions extrapolate to zero at trajectories of nearly the same length, log(trajectory/$\tau_{fit,med}$) = 3.75 and 3.82, respectively. This suggests full ergodicity recovery at ~6,000 $\tau_{fit,med}$.

1. Loudet A, Burgess K (2007) BODIPY dyes and their derivatives: Syntheses and spectroscopic properties. *Chem Rev* 107(11):4891–4932.
2. Richert R (2005) On the dielectric susceptibility spectra of supercooled o-terphenyl. *J Chem Phys* 123(15):154502.
3. Berberan-Santos MN, Bodunov EN, Valeur B (2005) Mathematical functions for the analysis of luminescence decays with underlying distributions 1. Kohlrausch decay function (stretched exponential). *Chem Phys* 315(1-2):171–182.
4. Pollard H (1946) The representation of $e^{-x\lambda}$ as a Laplace integral. *Bull Am Math Soc* 52(10):908–910.
5. Provencher SW (1982) Contin: A general purpose constrained regularization program for inverting noisy linear algebraic and integral equations. *Comput Phys Commun* 27(3):229–242.

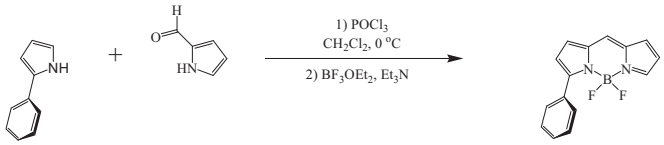

Fig. S1. Synthetic scheme for BODIPY268.

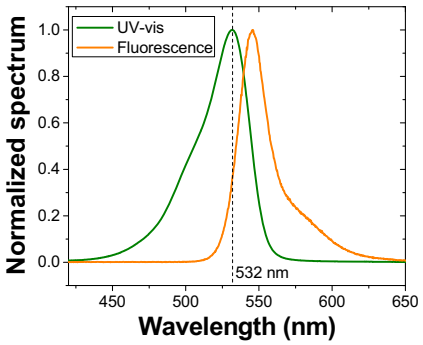

Fig. S2. Absorbance and fluorescence spectra of BODIPY268 in toluene. The vertical dashed line indicates the excitation wavelength used in the single-molecule measurements. Maximum excitation and emission wavelengths were determined to be 531.4 nm and 546.0 nm, respectively.

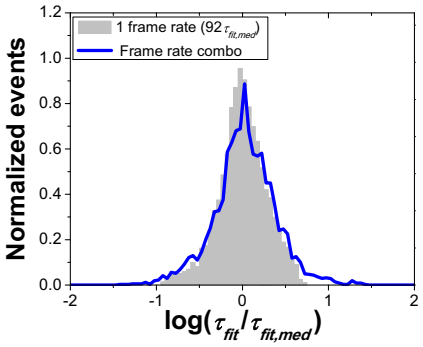

Fig. S3. Comparison of τ_{fit} distribution for single frame rate measurement (gray) and combined frame rate measurement (blue line).

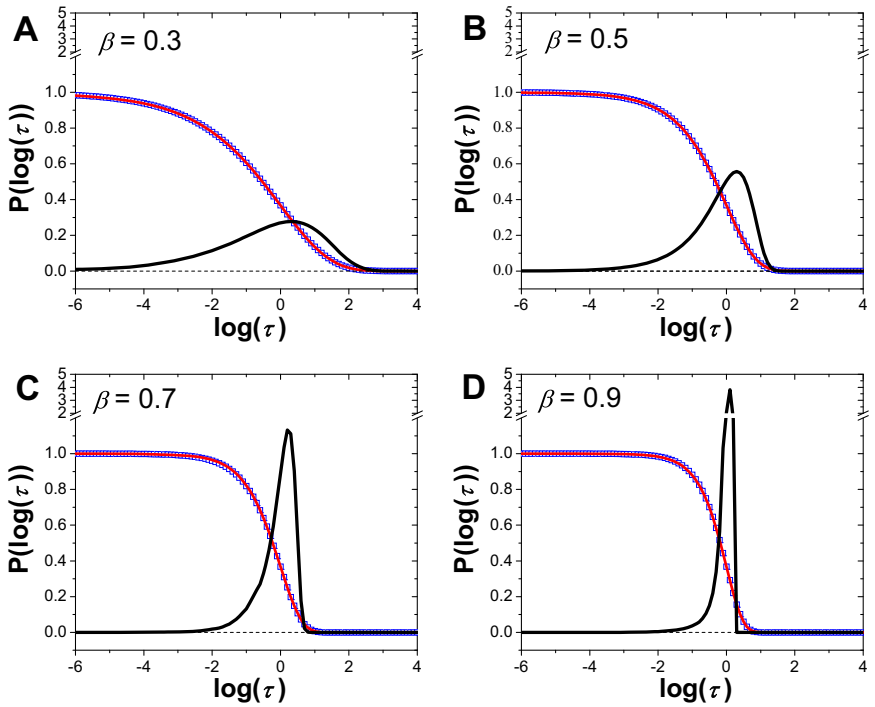

Fig. S4. Sample reference distributions generated by ILTs of stretched exponentials with different β values: (*A*) $\beta = 0.3$, (*B*) $\beta = 0.5$, (*C*) $\beta = 0.7$, and (*D*) $\beta = 0.9$. The blue dotted curve is the input stretched exponential decay function, and the red lines are decay functions regenerated from the obtained probability distribution function shown in black.

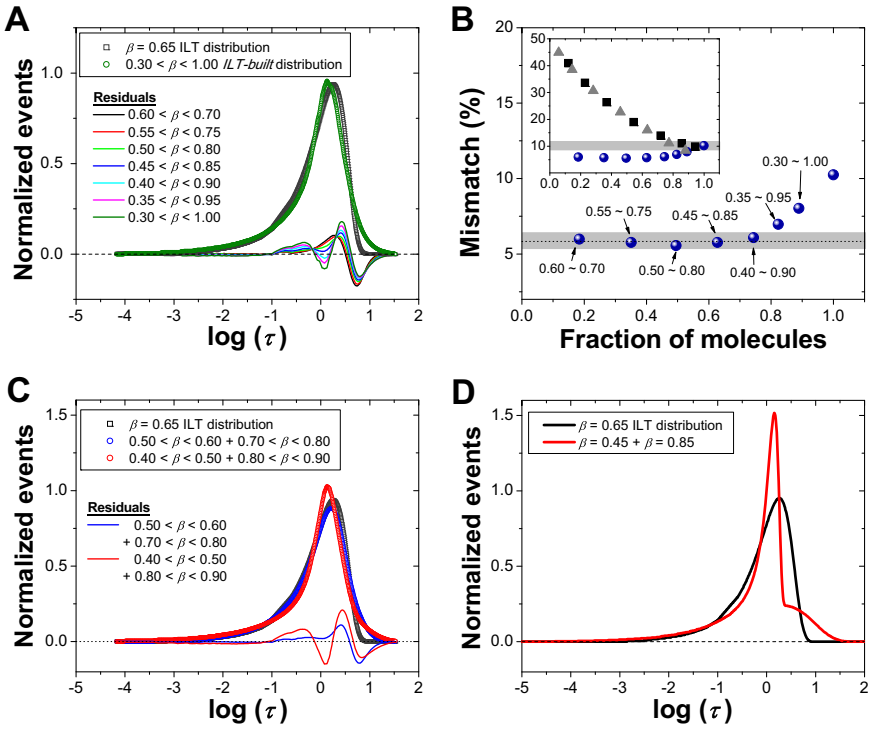

Fig. S5. (*A*) ILT distribution associated with $\beta = 0.65$ (black open symbols) and ILT-built distribution from molecules displaying β values from 0.30 to 1.00 (open green symbols). Solid lines are residuals from subtracting ILT-built distributions produced from molecules with given β values from the reference ILT distribution of $\beta = 0.65$. (*B*) Area mismatch calculated using the residuals shown in *A*. *Inset* shows this same area mismatch as well as mismatch for molecules when retaining those with the lowest (triangles) and highest (squares) β values; for example, the left-most triangle (square) represents molecules with $\beta = 0.30$–0.35 ($\beta = 0.95$–1.05), the second triangle (square) represents molecules with $\beta = 0.30$–0.45 ($\beta = 0.85$–1.05), and the right-most triangle (square) represents molecules with $\beta = 0.30$–0.85 ($\beta = 0.35$–1.05). (*C*) ILT distribution associated with $\beta = 0.65$ (black open symbols) and ILT-built distributions from molecules displaying β in particular ranges but excluding the middle of the distribution (blue and red symbols). Solid lines are residuals from subtracting ILT-built distributions produced from molecules with given β values from the reference ILT distribution of $\beta = 0.65$. (*D*) ILT distribution associated with $\beta = 0.65$ (black) and distribution constructed by a simple linear addition of ILT distributions constructed from β higher and lower than the ensemble β value.

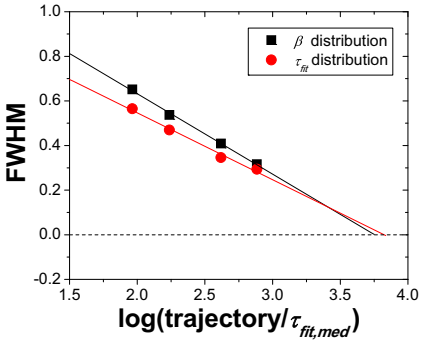

Fig. S6. The dependence of FWHM of β and τ_{fit} distributions with trajectory length as shown in Fig. 3. Lines are linear fits to the data.

Table S1. Number of molecules, median values from fits to stretched exponentials (τ_c, τ_{fit}, β), median survival time, and frame rate at each temperature for each trajectory set

	243 K	244.5 K	246 K	247.5 K	249 K	Combined	$415\tau_{fit,med}$ set (248 K)	$765\tau_{fit,med}$ set (248 K)
$92\tau_{fit,med}$ trajectory set								
Number of molecules	770	771	1,437	1,910	1,162	6,050		
Median τ_c, s	200.5	62.5	18.5	5.1	1.9			
Median τ_{fit}, s	135.6	44.7	12.6	3.6	1.3			
Median β	0.80	0.75	0.74	0.73	0.71	0.74		
Median trajectory, $\tau_{fit,med}$	58	75	90	97	133	92		
Median frame rate, frames per τ_{fit}	18.1	17.9	15.8	18.1	16.0	17.1		
FWHM (from τ_c distribution)	0.70	0.68	0.65	0.56	0.60	0.64		
β_{QE}	0.67	0.69	0.66	0.67	0.64	0.67		
$173\tau_{fit,med}$ trajectory set								
Number of molecules	1,119	1,285	1,057	1,152	1,225	5,838		
Median τ_c, s	228.1	66.9	22.4	3.8	1.9			
Median τ_{fit}, s	149.5	44.9	15.2	2.6	1.3			
Median β	0.67	0.66	0.68	0.68	0.65	0.67		
Median trajectory, $\tau_{fit,med}$	164	179	158	166	202	173		
Median frame rate, frames per τ_{fit}	15.0	15.0	15.2	13.0	13.0	14.1		
FWHM (from τ_c distribution)	0.49	0.48	0.47	0.48	0.43	0.47		
β_{QE}	0.63	0.63	0.64	0.63	0.64	0.63		
$415\tau_{fit,med}$ and $765\tau_{fit,med}$ trajectory sets								
Number of molecules							2,192	1,148
Median τ_c, s							3.8	3.9
Median τ_{fit}, s							2.5	2.5
Median β							0.62	0.61
Median trajectory, $\tau_{fit,med}$							415	765
Median frame rate, frames per τ_{fit}							12.4	12.6
FWHM (from τ_c distribution)							0.36	0.30
β_{QE}							0.61	0.61

FWHM values are best fits to the Gaussian distribution of $\log(\tau_c)$, and β_{QE} are the best-fit β values obtained from fitting the QE ACFs. The $173\tau_{fit,med}$ data are shown in Figs. 1 and 2, while all data sets are included in Figs. 3 and 4. The $415\tau_{fit,med}$ and $765\tau_{fit,med}$ trajectory sets are from the same 15,000 frame movie, analyzing molecules that survived through 2,000 and 7,000 frames, respectively.